Energy Efficiency Optimization for Backscatter Enhanced NOMA Cooperative V2X Communications Under Imperfect CSI

Wali Ullah Khan, *Member, IEEE*, Muhammad Ali Jamshed, *Member, IEEE*, Eva Lagunas, *Senior Member, IEEE*, Symeon Chatzinotas, *Senior Member, IEEE*, Xingwang Li, *Senior Member, IEEE*, and Björn Ottersten, *Fellow, IEEE*

***Abstract*— Automotive-Industry 5.0 will use beyond fifth-generation (B5G) technologies to provide robust, computationally intelligent, and energy-efficient data sharing among various onboard sensors, vehicles, and other devices. Recently, ambient backscatter communications (AmBC) have gained significant interest in the research community for providing battery-free communications. AmBC can modulate useful data and reflect it towards near devices using the energy and frequency of existing RF signals. However, obtaining channel state information (CSI) for AmBC systems would be very challenging due to no pilot sequences and limited power. As one of the latest members of multiple access technology, non-orthogonal multiple access (NOMA) has emerged as a promising solution for connecting large-scale devices over the same spectral resources in B5G wireless networks. Under imperfect CSI, this paper provides a new optimization framework for energy-efficient transmission in AmBC enhanced NOMA cooperative vehicle-to-everything (V2X) networks. We simultaneously minimize the total transmit power of the V2X network by optimizing the power allocation at BS and reflection coefficient at backscatter sensors while guaranteeing the individual quality of services. The problem of total power minimization is formulated as non-convex optimization and coupled on multiple variables, making it complex and challenging. Therefore, we first decouple the original problem into two sub-problems and convert the nonlinear rate constraints into linear constraints. Then, we adopt the iterative sub-gradient method to obtain an efficient solution. For comparison, we also present a conventional NOMA cooperative V2X network without AmBC. Simulation results show the benefits of our proposed AmBC enhanced NOMA cooperative V2X network in terms of total achievable energy efficiency.**

***Index Terms*— Beyond 5G, ambient backscatter communications (AmBC), non-orthogonal multiple access (NOMA), vehicle-to-everything (V2X), imperfect channel state information (CSI).**

Manuscript received 4 January 2022; revised 28 April 2022 and 15 June 2022; accepted 22 June 2022. An earlier version of this paper was presented at the IEEE VTC'2022-Spring, Helsinki, Finland, in June 2022 [1]. The Associate Editor for this article was H. Lv. *(Corresponding author: Wali Ullah Khan.)*

Wali Ullah Khan, Eva Lagunas, Symeon Chatzinotas, and Björn Ottersten are with the Interdisciplinary Center for Security, Reliability and Trust (SnT), University of Luxembourg, 1855 Luxembourg City, Luxembourg (e-mail: waliullah.khan@uni.lu; eva.lagunas@uni.lu; symeon.chatzinotas@uni.lu; bjorn.ottersten@uni.lu).

Muhammad Ali Jamshed is with the James Watt School of Engineering, University of Glasgow, Glasgow G12 8QQ, U.K. (e-mail: muhammadali.jamshed@glasgow.ac.uk).

Xingwang Li is with the School of Physics and Electronic Information Engineering, Henan Polytechnic University, Jiaozuo 454099, China (e-mail: lixingwangbupt@gmail.com).

Digital Object Identifier 10.1109/TITS.2022.3187567

I. Introduction

BEYOND fifth-generation (B5G) transportation systems will improve traffic efficiency, control, reliability, and passenger safety [2]–[4]. In this regard, vehicle-to-everything (V2X) communication such as vehicle-to-vehicle, vehicle-to-pedestrian, vehicle-to-infrastructure, and vehicle-to-air is one of the promising technologies to make it possible [5], [6]. V2X is expected to support diverse quality of services (QoS), massive connectivity, offer very low latency, and energy-efficient communication [7]. Recently, 3rd generation partnership project (3GPP) is also working on different V2X solutions regarding public safety [8]. However, there still exist various research challenges in the current transportation systems that need to be investigated [9]. One of the critical issues is the massive connectivity in B5G V2X networks which might not be possible through the existing orthogonal spectrum access resources, resulting in traffic and data congestion [10]. Another challenge is the fair and efficient resource allocation among large scale devices [11], [12]. Thus, new spectrum access technologies would be required to provide high spectral efficiency and support massive connectivity in B5G V2X networks.

Recently, non-orthogonal multiple access (NOMA) using power domain multiplexing has emerged as one of the top air interface technology due to its high spectral efficiency and low latency [13]. One of the main features of NOMA is to accommodate multiple devices over the same spectrum resource simultaneously [14]. It can be achieved through two different techniques, i.e., superposition coding (SC) and successive interference cancellation (SIC). In particular, SC is used on the transmitter side to superimpose multiple signals over the same spectrum using different transmit power, and SIC is then applied on the receiver side to decode different signals [15]. It is important to note that the power allocation for different signals over the same spectrum is done based on the channel conditions [16]. A device with poor channel conditions will assign a high transmit power, and the one with good channel conditions will allocate a low transmit power [17]. It guarantees the QoS of weak devices and also ensures fairness among different devices in the network [18]. The explosive growth of wireless devices in V2X communication and their diverse QoS requirements will consume huge energy [19]–[21]. Recently, the research community in

academia and industry is striving for various energy-efficient solutions to ease this critical situation [22]. Some of the possible solutions are to utilize the solar energy, conversion of vehicles to electric and use the existing ambient RF signals for communication among different vehicles.

Ambient backscatter communication (AmBC) has recently gained tremendous attention due to its ability to use the existing RF signals for modulating and reflecting useful information [23]. The fundamental concept of AmBC is to design a device that can harvest energy from the existing RF signals to operate its circuit by modulating and reflecting own information [24], [25]. This feature of the AmBC system make it the leading candidate technology towards battery-free communication in B5G era [23]. Most of these devices are sensors that act as a tag by reflecting the existing RF signal towards near devices without exploiting any oscillatory circuity [26]. From the last couple of years, the performance of these devices in various communication scenarios using conventional OMA technology has been extensively explored in the literature [27]–[30].

A. Recent Literature

Various research works have recently been investigated the performance of AmBC in NOMA networks. For example, Zhang *et al.* have proposed a AmBC enhanced downlink NOMA system to investigate the outage probability and ergodic sum rate [31]. The work in [32] have studied the system outage probability and throughput in AmBC enhanced NOMA communication. By integrating AmBC enhanced NOMA to air network, the authors of [33] have enhanced the successive bit rate while optimized the flight time and altitude of unmanned aerial vehicle. In another study, Chen *et al.* have investigated the expected sum capacity and outage probability of cooperative AmBC enhanced NOMA network [34]. Nazar *et al.* have provided AmBC enhanced NOMA framework to investigate the closed expression for bit error rate and bakscatter coverage [35]. To analyse the secrecy of the system, Li *et al.* have computed the closed expressions of outage and intercept probability for AmBC enhanced NOMA network [36]. Similar to [31], Raza *et al.* have proposed a massive machine type communication based on AmBC enhanced NOMA system and investigated the outage probability and ergodic rate [37]. To improve the reliability and security of maritime transmission system, Li *et al.* [38] have calculated the outage and intercept probability in AmBC enhanced NOMA internet-of-vehicle network. Ding *et al.* have provided AmBC enhanced NOMA and wireless power transfer enhanced NOMA systems and investigate the outage probability and ergodic rate [39]. The authors of [40] have studied the impact of imperfect SIC, channel estimation error and residual hardware impairments on security and reliability performance of AmBC enhanced NOMA system. Further, the performance of AmBC enhanced NOMA with intelligent reflecting surfaces has also investigated by Le *et al.* in the form of outage probability, throughput and capacity [41].

Researchers have also studied different resource allocation, and optimization frameworks in AmBC enhanced NOMA networks. For example, Khan *et al.* [42] have presented a joint optimization framework for AmBC enhanced multi-cell NOMA network. They maximize the total achievable energy efficiency by optimizing the total transmit power of the base station (BS), users' power allocation, and the backscatter sensor's reflection coefficient under imperfect SIC decoding. To maximize the system throughput and fairness, the authors of [43] have jointly optimized the reflection coefficient, power and time allocation for full duplex AmBC enhanced NOMA network. In [44], authors have maximized the spectral efficiency of AmBC enhanced NOMA V2X network by jointly optimize the transmit power of BS and roadside units (RSUs). Ding *et al.* have showed the advantages of using NOMA as a multiple access technique compared to other OMA techniques in AmBC network [45]. The researchers of [46], [47] have provided a new optimization framework to maximize the sum rate of AmBC enhanced NOMA network under perfect and imperfect SIC decoding. Moreover, Xu *et al.* [48] have proposed a joint optimization framework for energy efficiency of AmBC enhanced NOMA network by allocating transmit power and designing reflection coefficient. To improve the secrecy in the presence of multiple non-colluding eavesdroppers, the works of [49], [50] have optimized resource allocation in single-cell and multi-cell AmBC enhanced NOMA network. Ding *et al.* [51] have provided an new optimization framework to improve the uplink transmission rate while mitigate the interference between downlink and uplink of AmBC enhanced NOMA network. Furthermore, Ahmed *et al.* [52] investigated the energy efficiency optimization problem in multi-cell AmBC enhanced NOMA network under imperfect SIC decoding. In [53], the authors have presented a joint optimization framework to maximize the secrecy rate of AmBC enhanced NOMA network with multiple eavesdroppers. Of late, the research in [54] has explored a spectral efficiency optimization problem for multi-cell AmBC enhanced NOMA network.

B. Motivation and Contributions

Despite extensive works on AmBC enhanced NOMA networks, the existing literature has not consider imperfect channel state information (CSI). In fact they consider perfect CSI in their proposed models, which is very challenging and hard in real vehicular systems. Besides that, most research works focus on non-vehicular and non-cooperative communications. To the best our knowledge, the problem of resource allocation for energy efficiency in AmBC enhanced NOMA cooperative V2X communication under imperfect CSI has not been considered previously. Motivated by this, we proposed a new optimization framework for energy efficiency in AmBC enhanced NOMA cooperative V2X network. In particular, we simultaneously optimize the transmit power of BS and RSUs while the reflection coefficient of backscatter sensor under imperfect CSI. We formulate the total transmit power minimization problem as non-convex and hard to solve jointly. Therefore, we first transform and decouple the original problem (denoted as $\mathcal{P}$) into two sub-problems, i.e., $\mathcal{P}1$ for first time slot (transmission from BS to RSUs) and $\mathcal{P}2$ for second time slot (transmission from RSUs to vehicles), respectively.

Then we adopt iterative sub-gradient method to obtain an efficient solution. The main contributions of this work can be summarized as

1) This paper proposes an energy-efficient optimization framework for AmBC enhanced NOMA cooperative V2X communication. In particular, we consider half duplex communication, where a BS transmit the superimposed signal to its serving RSUs in the first time slot following NOMA protocol. The RSUs act as relays, first decode the signal of BS and then forward to their associated vehicles in the second time slot. Meanwhile, the backscatter sensors also receive the signals of RSUs, modulate their own information and reflect towards vehicles. Thus, we simultaneously optimize the transmit power of BS and RSUs while the reflection coefficient of backscatter sensors under imperfect CSI. The objective is to minimize the total transmit power of V2X network while taking into account several practical constraints.
2) The problem of energy efficiency optimization is formulated as non-convex due to the imperfect CSI and co-channel interference. Moreover, our optimization problem is non-convex due to inter-cell interference and multiple optimization variables, making it very challenging to solve it directly. Therefore, an efficient way to solve the problem is to divide the original problem into two sub-problems. Then, we exploit the low-complex iterative sub-gradient method to obtain a sub-optimal yet efficient solution. In addition, we provide an algorithm to show different steps involve in the solution while also discussing its complexity.
3) Finally, we present the comprehensive numerical results based on Monte Carlo simulations. In the results, we characterize the efficiency of the proposed optimization framework based on sub-gradient algorithm. We demonstrate the impact of imperfect CSI on the total achievable energy efficiency of AmBC enhanced NOMA cooperative V2X network. We also show the effect of other key system parameters over the system performance such as total available transmit power, coverage of RSUs and circuit power consumption. In addition, we also provide the results of NOMA cooperative V2X communication without AmBC for comparison with the proposed framework.

The remainder of this paper is organized as follows. Section II discusses system model, various assumptions, and channel models at first time slot and second time slot. Section III explains and presents different constraints and problem formulation of total transmit power minimization. Section IV provides proposed solution based on iterative sub-gradient method. Section V presents simulation results and their discussion while Section VI concludes this paper with some future research directions. Various notations used in this paper are listed in Table I.

TABLE I
LIST OF NOTATIONS AND THEIR DEFINITION

Notation	Definition
x	Superimposed signal of BS.
$m \in \{1,2\}$	Represents RSU, i.e., R_m.
P	Transmit power of BS.
α_m	Power allocation coefficient of R_m.
x_m	Data symbol of R_m.
h_m	Denotes channel gain of R_m.
H_m	Denotes Rayleigh fading coefficient of R_m.
d_m	Distance between BS and R_m.
ζ	Data symbol of i-th IE over j-th BF.
$\hat{h}_m$	Estimated channel gain of R_m.
ϵ_m	Estimated channel error.
σ_ϵ^2	Variance of AWGN.
y_m	Received signal of R_m.
ϖ_m	Additive white Gaussian noise.
C_1, C_2	Data rate of R_1 and R_2.
t_1, t_2	First time slot and second time slot.
γ_1, γ_2	SINR of R_1 and R_2.
s_m	Superimposed signal of R_m.
Q_m	Transmit power of R_m
$i \in \{1,2\}$	Represent vehicle of R_m, i.e., $V_{1,m}$.
$\beta_{i,m}$	Power allocation coefficient of $V_{i,m}$.
$s_{i,m}$	Data symbol of $V_{i,m}$.
B_m	Denotes backscatter tag in R_m.
z_m	Reflected data symbol of B_m.
$y_{i,m}$	Received signal of $V_{i,m}$.
$\hat{h}_{i,m}$	Estimated channel gain of $V_{i,m}$.
ξ	Reflection coefficient of B_m.
$\hat{h}_{i,m}^b$	Estimated channel gain between B_m of $V_{i,m}$.
$\hat{h}_{b,m}$	Estimated channel gain between B_m of R_m.
$\varpi_{i,m}$	AWGN of $V_{i,m}$.
$C_{1,m}, C_{2,m}$	Data rate of $V_{1,m}$ of $V_{2,m}$.
$I_{i,m}^{m'}$	Inter-RSU interference.
$\gamma_{1,m}, \gamma_{2,m}$	SINR of $V_{1,m}$ of $V_{2,m}$.
$\bar{C}$	End-to-end data rate.
$\bar{C}_{sum}$	End-to-end sum data rate.
C_{min}	Minimum required data rate.
P_{max}	Maximum power budget of BS.
Q_{max}	Maximum power budget of R_m.
L_1, L_2	Lagrangian function of (P1) and (P2).
ψ_1, ψ_2	Lagrangian multipliers of L_1 in (P1).
λ_1, λ_2	Lagrangian multipliers of L_1 in (P1).
$\eta_{1,m}, \eta_{2,m}, \mu_{i,m}$	Lagrangian multipliers of L_2 in (P2).
ζ_m, υ_m	Lagrangian multipliers of L_2 in (P2).
δ	Non-negative step size.
t	Iteration index.

II. SYSTEM AND CHANNEL MODELS

Consider an AmBC enhanced NOMA cooperative V2X communication, as illustrated in Figure 1. In the proposed model, we consider a half-duplex communication such that the data transmission from source to destination is completed in two time slots using NOMA protocol. More specifically, a BS transmits the superimposed signal to multiple RSUs in the first time slot. The RSUs first decode the signal of BS and then forward it to their associated vehicles in the second time slot. Meanwhile, the backscatter sensors also receive the signals of RSUs and reflect it toward vehicles by adding some useful information. In this work, we make the following assumptions:

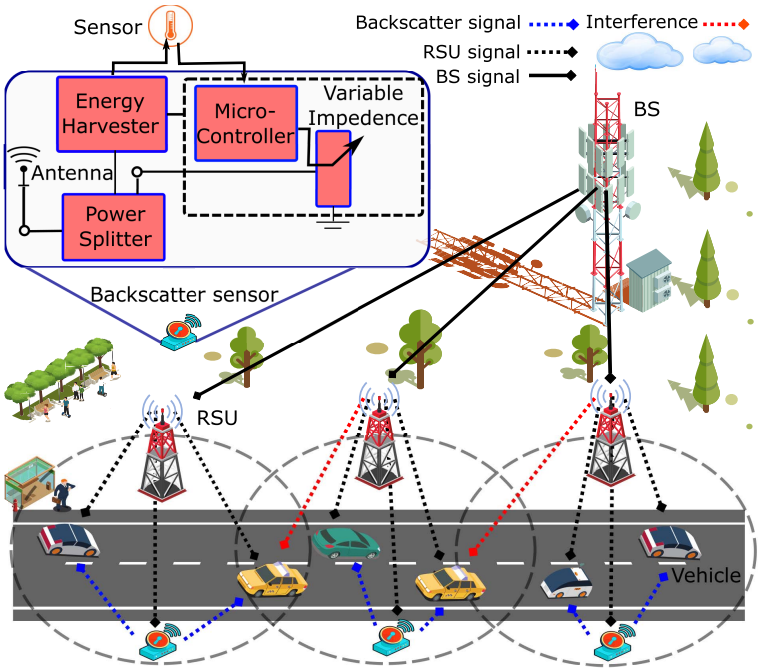

Fig. 1. System model of AmBC enhanced NOMA cooperative V2X communication.

1) The direct link from BS to vehicles and backscatter sensors is missing due to large distance and shadowing; 2) The BS, RSUs, backscatter sensors, and vehicles are using omnidirectional antenna; 3) Due to the mobility of vehicles, the CSI is changing rapidly, and it is very challenging to obtain it perfectly. Thus, we consider both perfect and imperfect SCI in the system; 4) The channels between different devices are independent and undergo Rayleigh fading. In the following, we discuss the channel models and signal to interference plus noise ratios at first and second time slot.

A. First Time Slot (transmission From BS to RSUs)

In the first time slot, transmission between BS and RSUs[1] takes place. A superimposed signal that BS transmits (denoted as x) can be expressed as

$$x = \sum_{m=1}^{2} \sqrt{P\alpha_m} x_m, \tag{1}$$

where P is the transmit power of BS and α_m denotes the power allocation coefficient of RSU (denoted as R_m), for $m \in \{1, 2\}$. Moreover, x_m represents the unit power signal of R_m. The channel from BS to R_m can be modeled as

$$h_m = H_m \times d_m^{\frac{-\zeta}{2}}, \tag{2}$$

where H_m is the Rayleigh fading coefficient, d_m denotes the distance from BS to R_m and ζ represents the pathloss exponent. In this work, we consider errors in channel estimation, hence the CSI is imperfect. Using the minimum mean square error (MMSE) model, the channel of R_m from the BS is estimated as

$$h_m = \hat{h}_m + \epsilon_m, \tag{3}$$

where $\hat{h}_m$ is the estimated channel gain of h_m with variance $\sigma^2_{\hat{h}_m}$ and ϵ_m represents the estimated channel error with zero mean and $\sigma^2_{\epsilon_m}$ variance. For the convenience of discussion, the case of constant estimation error ($\sigma^2_{\epsilon_m} = \sigma^2_{\epsilon}$) for all channels is considered in this work. It is important to note that both $\hat{h}_m$ and ϵ_m are uncorrelated. The signal that R_m receives from BS can be expressed as

$$y_m = \hat{h}_m x + \epsilon x + \varpi_m, , \tag{4}$$

where ϖ_m is the additive white Gaussian noise (AWGN) with zero mean and σ^2 variance. We assume that the channel gains of RSUs are arranged as $\hat{h}_1 > \hat{h}_2$. Therefore, R_1 can apply SIC to decode its signal while R_2 cannot apply SIC and decode its signal by treating the signal of R_1 as a noise. Based on these observations, the data rate C_1 and C_2 can be written as $C_1 = t_1 W \log_2(1 + \gamma_1)$ and $C_2 = t_1 W \log_2(1 + \gamma_2)$, where t_1 shows the first transmission slot which should be equal to 1/2 and W is the bandwidth. The terms γ_1 and γ_2 are the signal-to-interference-plus-noise-ratio (SINR) which can be stated as

$$\gamma_1 = \frac{|\hat{h}_1|^2 P\alpha_1}{P\sigma^2_{\epsilon}(\alpha_1 + \alpha_2) + \sigma^2}. \tag{5}$$

$$\gamma_2 = \frac{|\hat{h}_2|^2 P\alpha_2}{|\hat{h}_2|^2 P\alpha_1 + P\sigma^2_{\epsilon}(\alpha_1 + \alpha_2) + \sigma^2}. \tag{6}$$

B. Second Time Slot (transmission From RSUs to vehicles)

In this time slot, a transmission between RSUs and vehicles takes place. The RSUs first regenerate the superimposed signal and then forward it. The signal that R_m

[1]To reduce the SIC decoding complexity and inter-RSU interference, we consider two RSUs associated with BS at any given time such that each RSU serves two vehicles.

transmits (denoted as s_m) to its associated vehicles can be written as

$$s_m = \sum_{i=1}^{2} \sqrt{Q_m \beta_{i,m}} s_{i,m}, \tag{7}$$

where Q_m is the transmit power of R_m, $\beta_{i,m}$ represents the power allocation coefficient of the vehicle (denoted as $V_{i,m}$), for $i \in \{1, 2\}$ and $s_{i,m}$ denotes the unit power signal of $V_{i,m}$. The channels used in this time slot are modeled and estimated similar to the first time slot. However, for the simplicity, we omit all the steps here and denote the channel from R_m to $V_{i,m}$ as $\hat{h}_{i,m}$. Without loss of generality, we assume that the channel gains of $V_{1,m}$ is stronger than $V_{2,m}$, i.e., $|\hat{h}_{1,m}|^2 > |\hat{h}_{2,m}|^2$.

During the transmission in the second time slot, a backscatter sensor in the geographical area of R_m (stated as B_m) also receives the superimposed signal s_m from R_m. B_m first harvests energy from s_m, then modulate its own message z_m and reflect it towards $V_{i,m}$, where $\mathbb{E}[|z_m|^2] = 1$ and $\mathbb{E}[.]$ represents the expectation operation. Due to the short transmission range, we assume that the interference of a backscatter transmission to nearby cells is almost negligible and it can be safely ignored. Since we consider imperfect CSI, therefore the signal that $V_{i,m}$ receives from R_m can be expressed as

$$y_{i,m} = \hat{h}_{i,m} s_m + \sqrt{\xi_m} \hat{h}^b_{i,m} \hat{h}_{b,m} s_m z_m + \epsilon s_m + \epsilon \sqrt{\xi_m} + \varpi_{i,m}, \tag{8}$$

where ξ_m is the reflection coefficient of B_m and $\hat{h}^b_{i,m}$ denotes the channel gain between B_m and $V_{i,m}$. Further, $\hat{h}_{b,m}$ represents the channel gain between R_m and B_m while $\varpi_{i,m}$ states the AWGN. Based on the received signal in (8), the data rate of $V_{1,m}$ and $V_{2,m}$ cab be formulated as $C_{1,m} = t_2 W \log_2(1+\gamma_{1,m})$ and $C_{2,m} = t_2 W \log_2(1+\gamma_{2,m})$. Where t_2 represents the second transmission slot while $\gamma_{1,m}$ and $\gamma_{2,m}$ is the SINR of $V_{1,m}$ and $V_{2,m}$ as

$$\gamma_{1,m} = \frac{Q_m \beta_{1,m} (|\hat{h}_{1,m}|^2 + \xi_m |\hat{h}^b_{1,m}|^2 |\hat{h}_{b,m}|^2)}{\sigma^2_\epsilon (Q_m (\beta_{1,m} + \beta_{2,m}) + \xi_m) + I^{m'}_{1,m} + \sigma^2}. \tag{9}$$

$$\gamma_{2,m} = \frac{Q_m \beta_{2,m} (|\hat{h}_{2,m}|^2 + \xi_m |\hat{h}^b_{2,m}|^2 |\hat{h}_{b,m}|^2)}{\Pi_{2,m} + \sigma^2_\epsilon (Q_m (\beta_{1,m} + \beta_{2,m}) + \xi_m) + I^{m'}_{2,m} + \sigma^2}. \tag{10}$$

where in both equations, the term $\xi_m |\hat{h}^b_{1,m}|^2 |\hat{h}_{b,m}|^2$ and $\xi_m |\hat{h}^b_{2,m}|^2 |\hat{h}_{b,m}|^2$ in the nominator refer to the useful signals at vehicles received from the backscatter sensors. Furthermore, $\Pi_{2,m} = Q_m \beta_{1,m} (|\hat{h}_{2,m}|^2 + \xi \hat{h}^b_{2,m} \hat{h}_{b,m})$ is the interference due to NOMA transmission, and $I^{m'}_{i,m} = |\hat{h}^{m'}_{i,m}|^2 Q_{m'}$ is the inter-RSU interference due to the same channel reuse. Following decode-and-forward protocol at RSUs, the end-to-end rate can be calculated as

$$\bar{C} = \frac{1}{2} \min\{C_m, C_{i,m}\}. \tag{11}$$

Accordingly, the sum rate of the proposed cooperative V2X network can be computed as

$$\bar{C}_{sum} = \sum_{m=1}^{2} \sum_{i=1}^{2} \frac{1}{2} \min\{C_m, C_{i,m}\}. \tag{12}$$

III. Problem Formulation

This work aims to provide energy-efficient communication in AmBC-enhanced NOMA cooperative V2X communication by optimizing various network resources, i.e., power allocation at BS and RSUs, while reflection coefficient at backscatter sensors. The total transmit power of the system can be written as

$$\sum_{m=1}^{2} P \alpha_m + \sum_{m=1}^{2} \sum_{i=1}^{2} Q_m \beta_{i,m}. \tag{13}$$

The objective is to minimize the total power consumption while considering various practical constraints, which can be expressed as follows.

- *Minimum data rate constraints:* To ensure the minimum data rate at both time slots, the minimum data rate should satisfy as

$$\sum_{m=1}^{2} C_m \geq C_{min}, \tag{14}$$

$$\sum_{m=1}^{2} \sum_{i=1}^{2} C_{i,m} \geq C_{min}, \tag{15}$$

  where C_{min} is the minimum rate requirement for quality of services.
- *Power limit constraint:* To limit the total power at both time slots, the transmit power at BS and RSUs should satisfy as

$$0 \leq \sum_{m=1}^{2} P \alpha_{\leq} P_{max}, \tag{16}$$

$$0 \leq \sum_{m=1}^{2} \sum_{i=1}^{2} Q_m \beta_{i,m} \leq Q_{max}, \tag{17}$$

  where P_{max} and Q_{max} denote the maximum power that BS and RSUs can transmit with.
- *Reflection coefficient constraint:* To control the reflection power of backscatter sensors in the second time slot, its reflection coefficient should be ranging between zero and one as

$$0 \leq \xi_m \leq 1, m \in \{1, 2\}. \tag{18}$$

The formulation of the power minimization problem can also be represented as

$$\mathcal{P} \min_{\alpha_m, \beta_{i,m}, \xi_m} \left\{ \sum_{m=1}^{2} P \alpha_m + \sum_{m=1}^{2} \sum_{i=1}^{2} Q_m \beta_{i,m} \right\}$$

$$s.t. \quad \mathcal{A}1 : \sum_{m=1}^{2} C_m \geq C_{min},$$

$$\mathcal{A}2 : \sum_{i=1}^{2} C_{i,m} \geq C_{min}, m \in \{1, 2\},$$

$$\mathcal{A}3 : \sum_{m=1}^{2} P \alpha_m \leq P_{max},$$

$$\mathcal{A}4: \sum_{m=1}^{2} \alpha_m \leq 1,$$
$$\mathcal{A}5: \sum_{i=1}^{2} Q_m \beta_{i,m} \leq Q_{max}, m \in \{1,2\},$$
$$\mathcal{A}6: \sum_{i=1}^{2} \beta_{i,m} \leq 1, m \in \{1,2\},$$
$$\mathcal{A}7: 0 \leq \xi_m \leq 1, m \in \{1,2\}, \quad (19)$$

where the objective of $\mathcal{P}$ is to minimize the total transmit power of AmBC-enhanced NOMA cooperative V2X communication. Constraints $\mathcal{A}1$ and $\mathcal{A}2$ ensure the minimum data rate, where C_{min} shows its threshold. Constraints $\mathcal{A}3$ and $\mathcal{A}5$ limit the transmit power of BS and RSUs, where P_{max} and Q_{max} are the maximum power that BS and RSU can transmit with at the given time. Constraints $\mathcal{A}4$ and $\mathcal{A}6$ describe the power allocation according to NOMA protocol. Constraint $\mathcal{A}7$ controls the reflection coefficient of backscatter sensors. We can see that the problem $\mathcal{P}$ is non-convex due to $\mathcal{A}1$ and $\mathcal{A}2$, making it very challenging to solve. Thus, we first transform and decouple it into two sub-problems and then employ the sub-gradient method to obtain an efficient solution.

IV. Proposed Energy-Efficient Solution

The problem $\mathcal{P}$ is coupled on multiple variables which makes it very complex. Thus, we first transform and decouple it into two sub-problems, i.e., i) power allocation at BS; 2) power allocation at RSUs and reflection coefficient at backscatter sensors. Then, we adopt iterative sub-gradient method to obtain sub-optimal yet efficient solution [55].

A. Power Allocation for BS

Here we optimize the power allocation of BS at first time slot for the fixed transmit power of RSUs and reflection coefficient of backscatter sensor at second time slot. By setting this, the original problem in (19) can be reformulated as

$$\begin{aligned}\mathcal{P}1 \min_{\alpha_1,\alpha_2}\ & P(\alpha_1+\alpha_2)\\ s.t.\ & \mathcal{A}8: |\hat{h}_1|^2 P\alpha_1 \geq (2^{C_{min}}-1)\\ & (P\sigma_\epsilon^2(\alpha_1+\alpha_2)+\sigma^2),\\ & \mathcal{A}9: |\hat{h}_2|^2 P\alpha_2 \geq (2^{C_{min}}-1)\times\\ & (|\hat{h}_2|^2 P\alpha_1 + P\sigma_\epsilon^2(\alpha_1+\alpha_2)+\sigma^2),\\ & \mathcal{A}10: P(\alpha_1+\alpha_2) \leq P_{max},\\ & \mathcal{A}11: \alpha_1+\alpha_2 \leq 1, \end{aligned} \quad (20)$$

where the objective of $\mathcal{P}1$ is to minimize the transmit power of BS. Constraint $\mathcal{A}8$ and constraint $\mathcal{A}9$ guarantee the minimum rate of R_1 and R_2, respectively. Constraint $\mathcal{A}10$ limits the transmit power of BS while constraint ($\mathcal{A}11$) is the power allocation limit of R_1 and R_2. To solve problem (P1), we employ the sub-gradient method, in which we first define a Lagrangian function as

$$\begin{aligned}L(\psi_1,\psi_2,\lambda_1,\lambda_2)&P(\alpha_1+\alpha_2)+\psi_1((2^{C_{min}}-1)\\ &(P\sigma_\epsilon^2(\alpha_1+\alpha_2)+\sigma^2)-|\hat{h}_1|^2P\alpha_1)+\psi_2((2^{C_{min}}-1)\\ &(|\hat{h}_2|^2P\alpha_1+P\sigma_\epsilon^2(\alpha_1+\alpha_2)+\sigma^2)-|\hat{h}_2|^2P\alpha_2)\\ &+\lambda_1(P(\alpha_1+\alpha_2)-P_{max})+\lambda_2((\alpha_1+\alpha_2)-1), \end{aligned} \quad (21)$$

where $\psi_1, \psi_2, \lambda_1, \lambda_2$ are the Lagrangian multipliers. After calculating the partial derivative, it can be written as

$$\begin{aligned}\frac{\partial L_1}{\partial \alpha_1} =\ & P+\lambda_1 P+(2^{C_{min}}-1)\psi_2(|\hat{h}_2|^2P+P\sigma_\epsilon^2)\\ &+\psi_1((2^{C_{min}}-1)P\sigma_\epsilon^2-|\hat{h}_1|^2P)+\lambda_2\alpha_1 \end{aligned} \quad (22)$$

$$\begin{aligned}\frac{\partial L_1}{\partial \alpha_2} =\ & P+\lambda_1 P+(2^{C_{min}}-1)P\psi_1\sigma_\epsilon^2\\ &+\psi_2((2^{C_{min}}-1)P\sigma_\epsilon^2-|\hat{h}_2|^2P)+\lambda_2\alpha_2 \end{aligned} \quad (23)$$

Next we iteratively update the power allocation coefficients and Lagrangian multipliers as

$$\alpha_1(t+1) = \left(\alpha_1(t)-\delta(t)\frac{\partial L_1}{\partial \alpha_1}\right)^+ \quad (24)$$

$$\alpha_2(t+1) = \left(\alpha_2(t)-\delta(t)\frac{\partial L_1}{\partial \alpha_2}\right)^+ \quad (25)$$

$$\begin{aligned}\psi_1(t+1) =\ & \big(\psi_1(t)-\delta(t)(|\hat{h}_1|^2P\alpha_1\\ &-(2^{C_{min}}-1)P\sigma_\epsilon^2(\alpha_1+\alpha_2)+\sigma^2)\big)^+ \end{aligned} \quad (26)$$

$$\begin{aligned}\psi_2(t+1) =\ & \big(\psi_2(t)-\delta(t)(|\hat{h}_2|^2P\alpha_2-(2^{C_{min}}-1)\\ &(|\hat{h}_2|^2P\alpha_1+P\sigma_\epsilon^2(\alpha_1+\alpha_2))+\sigma^2)\big)^+ \end{aligned} \quad (27)$$

$$\lambda_1(t+1) = \big(\lambda_1(t)-\delta(t)(P_{max}-P(\alpha_1+\alpha_2))\big)^+ \quad (28)$$

$$\lambda_2(t+1) = \big(\lambda_2(t)-\delta(t)(1-(\alpha_1+\alpha_2))\big)^+ \quad (29)$$

where t shows the iteration index and δ is the nonnegative step size. The above iterative process will continue until the required criterion is satisfied.

B. Power Allocation for RSUs and Reflection Coefficient for Backscatter Sensors

Now we calculate the transmit power of RSUs and reflection coefficient of backscatter sensors at second time slot. Therefore, for a given transmit power at BS, the original problem in (19) can be simplified as

$$\begin{aligned}\mathcal{P}2 \min_{\beta_{1,m},\beta_{2,m},\xi_m}\ & \sum_{m=1}^{2} Q_m(\beta_{1,m}+\beta_{2,m})\\ s.t.\quad & \mathcal{A}12: Q_m\beta_{1,m}(|\hat{h}_{1,m}|^2+\Omega_{1,m}) \geq (2^{C_{min}}-1)\\ & (\sigma_\epsilon^2(Q_m(\beta_{1,m}+\beta_{2,m})\\ & +\xi_m)+I_{1,m}^{m'}+\sigma^2), m\in\{1,2\},\\ & \mathcal{A}13: Q_m\beta_{2,m}(|\hat{h}_{2,m}|^2+\Omega_{2,m})\\ & \geq (2^{C_{min}}-1)(\Pi_{2,m}+\sigma_\epsilon^2(Q_m(\beta_{1,m}+\beta_{2,m})\\ & +\xi_m)+I_{2,m}^{m'}+\sigma^2), m\in\{1,2\},\\ & \mathcal{A}14: Q_m(\beta_{1,m}+\beta_{2,m}) \leq Q_{max}, m\in\{1,2\},\\ & \mathcal{A}15: \beta_{1,m}+\beta_{2,m} \leq 1, m\in\{1,2\},\\ & \mathcal{A}16: 0\leq\xi_m\leq 1, m\in\{1,2\}, \end{aligned} \quad (30)$$

where constraints $\mathcal{A}12$ and $\mathcal{A}13$ ensure the minimum rate of $V_{1,m}$ and $V_{2,m}$. Constraint $\mathcal{A}14$ and constraint $\mathcal{A}15$ control the transmit power of RSUs according to the NOMA protocol while $(A16)$ is the reflection coefficient constraint. Similar to $\mathcal{P}1$, here we also exploit the sub-gradient method. The Lagrangian function of $\mathcal{P}2$ can be defined as

$$\begin{aligned}L_2(\eta_{1,m},\eta_{2,m},\mu_{i,m},\zeta_m,\upsilon_m) &= Q_m(\beta_{1,m}+\beta_{2,m})\\ &+\eta_{1,m}((2^{C_{min}}-1)(\sigma_\epsilon^2(Q_m(\beta_{1,m}+\beta_{2,m})+\xi_m)\\ &+I_{1,m}^{m'}+\sigma^2)-Q_m\beta_{1,m}(|\hat{h}_{1,m}|^2+\xi_m|\hat{h}_{1,m}^b|^2|\hat{h}_{b,m}|^2))\\ &+\eta_{2,m}((2^{C_{min}}-1)(\Pi_{2,m}+\sigma_\epsilon^2(Q_m(\beta_{1,m}+\beta_{2,m})+\xi_m)\\ &+I_{2,m}^{m'}+\sigma^2)-Q_m\beta_{2,m}(|\hat{h}_{2,m}|^2+\xi_m|\hat{h}_{2,m}^b|^2|\hat{h}_{b,m}|^2))\\ &+\mu_m(Q_m(\beta_{1,m}+\beta_{2,m})-Q_{max})\\ &+\zeta_m((\beta_{1,m}+\beta_{2,m})-1)+\upsilon_m(\xi_m-1), m\in\{1,2\}, \quad (31)\end{aligned}$$

where $\eta_{1,m},\eta_{2,m},\mu_m,\zeta_m,\upsilon_m$ show the Lagrangian multipliers. Next we calculate the partial derivative of (31) with respect to $\beta_{1,m}$, $\beta_{2,m}$, and ξ_m which can be stated as

$$\begin{aligned}\frac{\partial L_2}{\partial\beta_{1,m}} &= Q_m(1-|\hat{h}_{1,m}|^2\eta_{1,m}-\xi_m|\hat{h}_{1,m}^b|^2|\hat{h}_{b,m}|^2\eta_{1,m}\\ &+(2_{min}^C-1)(\eta_{1,m}+\eta_2)\sigma_\epsilon^2+\mu_m) \quad (32)\\ \frac{\partial L_2}{\partial\beta_{2,m}} &= Q_m(1-|\hat{h}_{2,m}|^2\eta_{2,m}-\xi_m|\hat{h}_{2,m}^b|^2|\hat{h}_{b,m}|^2\eta_{2,m}\\ &+(2_{min}^C-1)(\eta_{1,m}+\eta_{2,m})\sigma_\epsilon^2+\mu_m) \quad (33)\\ \frac{\partial L_2}{\partial\xi_m} &= -\beta_{1,m}|\hat{h}_{1,m}^b|^2|\hat{h}_{b,m}|^2\eta_{1,m}Q_m-\beta_{2,m}|\hat{h}_{2,m}^b|^2|\hat{h}_{b,m}|^2\\ &\times\eta_{2,m}Q_m+(2_{min}^C-1)(\eta_1+\eta_{2,m})\sigma_\epsilon+\upsilon_m \quad (34)\end{aligned}$$

To calculate efficient values, we iteratively update the optimization variables along with Lagrangian multipliers as

$$\beta_{1,m}(t+1)=\left(\beta_{1,m}(t)-\delta(t)\frac{\partial L_2}{\partial\beta_{1,m}}\right)^+ \quad (35)$$

$$\beta_{2,m}(t+1)=\left(\beta_{2,m}(t)-\delta(t)\frac{\partial L_2}{\partial\beta_{2,m}}\right)^+ \quad (36)$$

$$\xi_m(t+1)=\left(\xi_m(t)-\delta(t)\frac{\partial L_2}{\partial\xi_m}\right)^+ \quad (37)$$

$$\begin{aligned}\eta_{1,m}(t+1) &= \Big(\eta_{1,m}(t)-\delta(t)\big(Q_m\beta_{1,m}(|\hat{h}_{1,m}|^2\\ &+\xi_m|\hat{h}_{1,m}^b|^2|\hat{h}_{b,m}|^2-(2^{C_{min}}-1)(\sigma_\epsilon^2(Q_m\\ &\times(\beta_{1,m}+\beta_{2,m})+\xi_m)+I_{1,m}^{m'}+\sigma^2)\big)\Big)^+ \quad (38)\\ \eta_{2,m}(t+1) &= \Big(\eta_{2,m}(t)-\delta(t)\big(Q_m\beta_{2,m}(|\hat{h}_{2,m}|^2+\xi_m\\ &|\hat{h}_{2,m}^b|^2|\hat{h}_{b,m}|^2-(2^{C_{min}}-1)(\Pi_{2,m}+\sigma_\epsilon^2(Q_m\\ &\times(\beta_{1,m}+\beta_{2,m})+\xi_m)+I_{2,m}^{m'}+\sigma^2)\big)\Big)^+ \quad (39)\end{aligned}$$

$$\mu_m(t+1)=\Big(\mu_m(t)-\delta(t)\big(Q_{max}-Q_m(\beta_{1,m}+\beta_{2,m})\big)\Big)^+ \quad (40)$$

$$\xi_m(t+1)=\Big(\xi_m(t)-\delta(t)\big(1-(\beta_{1,m}+\beta_{2,m})\big)\Big)^+ \quad (41)$$

$$\xi_m(t+1)=\Big(\xi_m(t)-\delta(t)\big(1-\xi_m\big)\Big)^+ \quad (42)$$

Algorithm 1 Energy Efficiency Optimization of V2X Network Using Sub-Gradient Method

INPUT ($P_{\max}$, σ_ϵ, $|\hat{h}_1|^2$, $|\hat{h}_2|^2$, $C_{\min}$, $|\hat{h}_{1,m}|^2$, $|\hat{h}_{2,m}|^2$, $\hat{h}_{1,m}^b|^2|$, $|\hat{h}_{2,m}^b|^2$, $|\hat{h}_{b,m}|^2$, and σ^2)
Set initial values of $\alpha_1=\alpha_2=0.5$;
Calculate initial NOMA interference using $|\hat{h}_2|^2P\alpha_1$;
Stage 1: Power allocation of hop 1 (First time slot transmission)
repeat
  Calculate α_1, α_2 and associated Lagrangian multipliers using (24)-(29) via iterative sub-gradient method;
  Re-calculate $|\hat{h}_2|^2P\alpha_1$;
until convergence
Calculate $Q_1=P\alpha_1$.
Calculate $Q_2=P\alpha_2$.
$Q_m=P(\alpha_1+\alpha_2)$.
Stage 2: Power allocation of hop 2 (Second time slot transmission)
For initial interference calculations set Q_m=$Q_{\max}/2$ $\forall m$;
Calculate initial inter-cell interference $I_{1,m}^{m'}$ and $I_{2,m}^{m'}$ $\forall m$;
Calculate initial NOMA interference $\Pi_{2,m}=Q_m\beta_{1,m}(|\hat{h}_{2,m}|^2+\xi\hat{h}_{2,m}^b\hat{h}_{b,m})$;
repeat
  for $m=1:2$ **do**
    Calculate $\beta_{1,m}$, $\beta_{2,m}$, ξ_m, and associated Lagrangian multipliers using (35)-(42) via iterative sub-gradient method;
    Calculate $Q_{m'}$ using $\beta_{1,m}$, $\beta_{2,m}$;
    Re-calculate $I_{1,m}^{m'}=|\hat{h}_{1,m}^{m'}|^2Q_{m'}$ and $I_{2,m}^{m'}=|\hat{h}_{2,m}^{m'}|^2Q_{m'}$;
    Re-calculate $\Pi_{2,m}=Q_m\beta_{1,m}(|\hat{h}_{2,m}|^2+\xi\hat{h}_{2,m}^b\hat{h}_{b,m})$
  end for
until convergence
OUTPUT α_1^*, α_2^*, $\beta_{1,1}^*$, $\beta_{1,2}^*$, $\beta_{2,1}^*$, $\beta_{2,2}^*$, ξ_1^*, and ξ_2^*.

where (35)-(42) are updated until the selection criterion is satisfied. In addition, a detailed steps involved in the proposed solution is also depicted in Algorithm 1.

C. Proposed Iterative Algorithm and Complexity Analysis

Here we discuss the detailed steps of the proposed iterative sub-gradient method as depicted in Algorithm 1. First, the proposed algorithm takes the channel parameters, i.e., $|\hat{h}_1|^2$, $|\hat{h}_{2,m}|^2$, $\hat{h}_{1,m}^b|^2|$, etc., rate requirements $C_{\min}$ and power constraints $P_{\max}$, as an input parameters. Then energy efficiency is optimized in two stages, i.e., at the first time slot (stage 1) and second time slot (stage 2), respectively. In stage 1, the proposed algorithm optimizes the energy efficiency by allocating efficient power for both RSUs at BS, where the power allocation coefficients and Lagrangian multipliers are iteratively updated. In stage 2, for the given parameters at stage 1, the proposed algorithm optimizes the energy efficiency of each RSU by allocating efficient power to their associated vehicles. In this stage, our proposed algorithm also optimizes the reflection coefficients of backscatter sensors. Note that in

TABLE II
SIMULATION PARAMETERS

Parameter	Value
Total power budget P_{tot}	45 dBm
Reflection coefficient	$0 \leq \xi \leq 1$
Channel type	Raleigh fading
RSU protocol	Decode-and-forward
Imperfect CSI (σ_ϵ)	0→0.01
Radius of BS	50 meters
Radius of RSU	20 meters
Channel realization	10^3
Minimum data rate $C_{\min}$	0.5 bps
Pathloss exponent (ζ)	4
Noise power density σ^2	-170 dBm
Bandwidth BW	1 MHz
Circuit power	5 dBm

both stages, the proposed algorithm ensures the QoS for RSUs and vehicles such that the value of $C_{\min}$ in both time slots is always satisfied.

Here we also analyze the complexity analysis of our proposed iterative two-stage energy-efficient optimization algorithm. In this work, the computational complexity of the proposed algorithm can be calculated in terms of iterations required for the convergence of various optimization variables. In stage 1 and stage 2, the iterative sub-gradient method is used to optimize the power allocation of BS and RSUs while the reflection coefficients of backscatter sensors. Generally, the worst-case computational complexity of Algorithm 1 will be similar to the worst-case computational complexity of the sub-gradient method. Specifically, the worst-case computational complexity of the sub-gradient method can be computed as $\mathcal{O}(1/\Lambda^2)$, where Λ is the number of iterations being used by the sub-gradient method to achieve the convergence.

V. NUMERICAL RESULTS AND DISCUSSION

Here we present and discuss the numerical results of the proposed AmBC enhanced NOMA cooperative V2X communication based on Monte Carlo simulations. In addition, we also compare the results with the conventional NOMA cooperative V2X communication without AmBC. This work calculates the achievable energy efficiency as bits/Joule (Mb/J), which is the ratio between the total transmission rate of the network and the total power consumption, including the circuit power. Unless mentioned all the parameters used for simulation are provided in Table II.

It is important to study the impact of errors in the channel estimation on the system performance by plotting the total energy efficiency of cooperative V2X network versus the increasing values of imperfect CSI in Figure 2 for both AmBC enhanced NOMA and conventional NOMA systems. As expected, the achievable energy efficiency of the proposed AmBC enhanced V2X communication and the conventional cooperative VEX communication decreases as the values of imperfect CSI increases. This is because the interference due to imperfect CSI increases resulting decrease in the total transmission rate of both networks. However, the proposed AmBC enhanced NOMA cooperative communication achieves higher energy efficiency than the benchmark pure NOMA

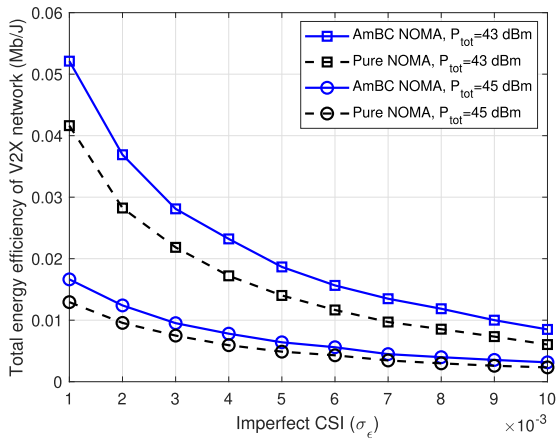

Fig. 2. Comparison of system total energy efficiency versus imperfect CSI by varying total available power budget, i.e., P_{tot}.

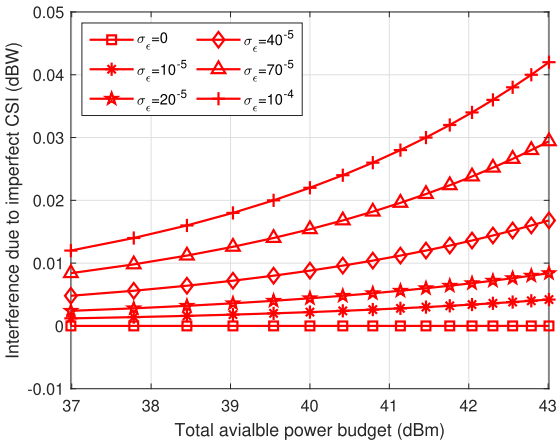

Fig. 3. Total causes interference due to imperfect SCI versus total available power budget by varying σ_ϵ.

cooperative V2X communication. For example, when the total transmit power of both networks is $P_{tot} = 43$ dBm and the value of σ_ϵ is 10^{-3}, the total energy efficiency of the proposed AmBC enhanced NOMA cooperative V2X communication is above 0.05 Mb/J. In comparison, the benchmark pure NOMA V2X communication can achieve only around 0.04 Mb/J. Moreover, similar trends can be seen when the total transmit power is $P_{tot} = 45$ dBm.

Next, we investigate the amount of interference caused by various values of imperfect CSI. In this regard, Figure 3 shows the interference due to imperfect CSI versus total available power budget for different values of σ_ϵ, i.e., $0, 10^{-5}, 20^{-5}, 40^{-5}, 70^{-5}, 10^{-4}$. Here we also show the result when the CSI is perfect. It can be evident that when the CSI is perfect, it causes zero interference for all values of the power budget. We can also observe that the interference is almost negligible for lower values of power budget and imperfect CSI. However, when the value of σ_ϵ increases, the interference due to imperfect CSI also increases. Furthermore, we can also see that the gap of interference among different curves increases as the total available power budget increase. It is because when the total available power budget increase, the system with high value of σ_ϵ produces high interference. This figure shows the

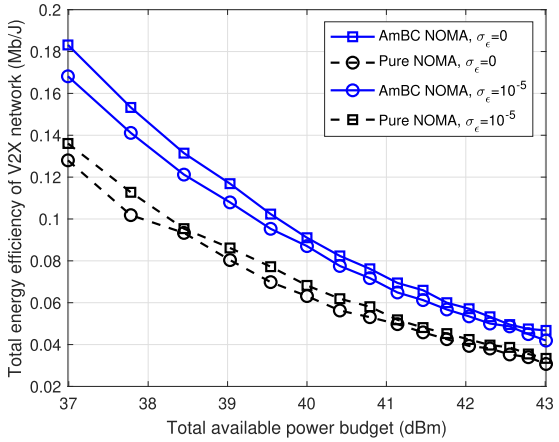

Fig. 4. Comparison of system total energy efficiency versus the total available power budget by varying values of σ_ϵ.

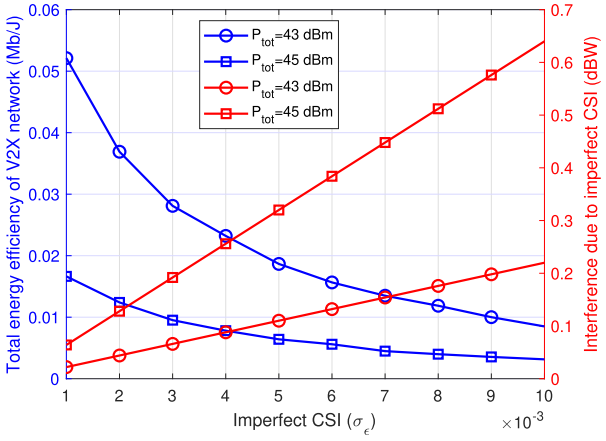

Fig. 5. Trade-off between system total energy efficiency and interference due to imperfect CSI by varying P_{tot}.

importance of CSI and how much it can affect a network's performance.

Figure 4 shows the impact of transmit power on achievable energy efficiency of the system. For this figure, the values of imperfect CSI are set as $\sigma_\epsilon = 0$ and $\sigma_\epsilon = 10^{-5}$, respectively, and the transmit power varies from 37 dBm to 43 dBm. For both AmBC enhanced NOMA and pure NOMA, the network under the perfect CSI achieves high energy efficiency compared to the imperfect CSI case. This reflects the importance of estimating efficient CSI in the energy-efficient transmission of both networks. We note that the total energy efficiency of both V2X communications follows bell-shaped curves under it grows first with the network total available power budget until the saturating point and then drops with further increase in the power budget. However, the performance gap between the proposed and benchmark network shows the advantages of integrating AmBC in NOMA cooperative V2X Communication.

Figure 5 describes the trade-off between total energy efficiency versus the interference when varying the values of imperfect CSI. For this plot, we set the total available power budget of V2X network is $P_{tot} = 43$ and $P_{tot} = 45$ while the values of σ_ϵ ranges between 10^{-3} and 100^{-3}, respectively. It is evident that the total energy efficiency of the proposed AmBC enhanced NOMA cooperative V2X communication decreases as the values of imperfect CSI, i.e., σ_ϵ, increase. At the same time, the amount of interference is increases for the increasing values of σ_ϵ. More specifically, for the lower values of σ_ϵ, the proposed V2X communication cause low interference and achieves high energy efficiency. Another point is to note that when the system operates with a lower available power budget, i.e., 43, it causes low interference and achieves very high energy efficiency.

Next, we show the impact of RSU coverage on the total energy efficiency of cooperative V2X communication for both AmBC enhanced NOMA and pure NOMA networks. Figure 6 plots the total energy efficiency versus the coverage area of RSUs. In this plot, we set the values of imperfect CSI as $\sigma_\epsilon = 0, 10^{-5}$. It can be observed that the achievable energy efficiency of both V2X networks is increasing with the decrease in the coverage area of RSUs. We can also see

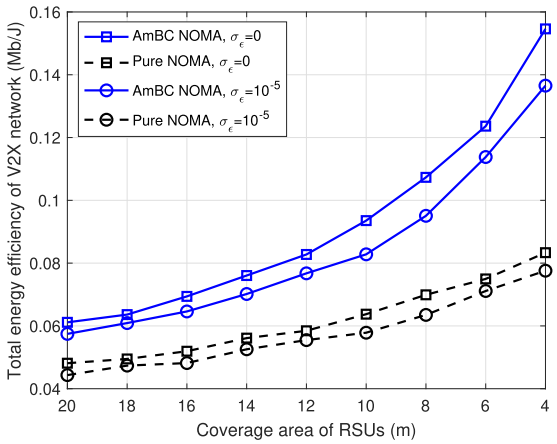

Fig. 6. Comparison of system total energy efficiency versus coverage area of RSUs by varying σ_ϵ.

that the perfect CSI systems achieve higher energy efficiency than the system with imperfect CSI. However, in perfect and imperfect CSI cases, the proposed AmBC enhanced NOMA cooperative V2X communication significantly outperforms the conventional pure NOMA cooperative V2X communication. Another important thing that should also be noted is that the gap of total energy efficiency between the proposed network and the benchmark network increases as the coverage area of RSUs decreases, which shows the effectiveness of AmBC in short-range transmission.

Last but not least, we check the impact of circuit consumption on the system's total energy efficiency for both networks. Figure 7 depicts the total energy efficiency versus the increasing values of circuit power consumption, where the values of σ_ϵ are 0 and 10^{-5}. As expected, the achievable energy efficiency of both networks reduces as the circuit consumption increases. However, for both $\sigma_E = 0$ and $\sigma_\epsilon = 10^{-5}$, the proposed AmBC enhanced NOMA cooperative V2X communication achieves very high energy efficiency compared to the pure NOMA V2X communication. For instance, when σ_ϵ is 10^{-5} and the circuit power consumption is 2 dBm, the proposed AmBC NOMA V2X network achieves above 0.02 Mb/J. On the other side, the conventional pure NOMA

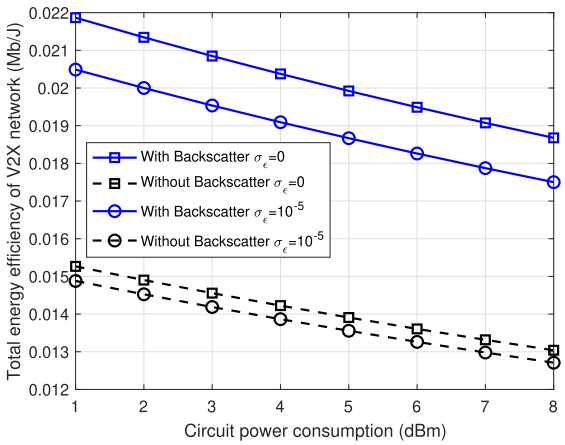

Fig. 7. Comparison of system total energy efficiency versus system circuit power consumption by varying σ_ϵ.

V2X network can only achieve 0.0145 Mb/J approximately for similar system parameters. This shows the importance of the proposed system using AmBC in such scenarios.

VI. Conclusion

AmBC and NOMA are promising technologies for providing high spectral and energy efficiency in future Automotive-Industry 5.0 communications. This work has investigated a new optimization problem for enhancing energy efficiency in AmBC enhanced NOMA cooperative V2X communication. In particular, the transmit power of BS and RSUs and the reflection coefficient of backscatter sensors have been optimized simultaneously under perfect/imperfect CSI errors. The problem of total transmit power minimization has been formulated as non-convex, which was very hard and complex. The original problem has been transformed and decoupled into two sub-problems, and then the iterative sub-gradient method has been adopted to obtain an efficient solution. Comprehensive simulation results have also been provided and discussed to show the advantages of AmBC enhanced NOMA cooperative V2X communication against the benchmark pure NOMA cooperative V2X communication.

Our proposed optimization framework can be further extended in multiple ways. For example, the considered system can be investigated under decode-and-forward and amplify-and-forward relaying protocols. The proposed system can also be studied when the RSUs operate in full-duplex such that the signal from BS to vehicles can be received in a one-time slot. Further, intelligent reflecting surfaces can be incorporated in the proposed model to replace the energy-constrained relays. These exciting yet explored topics will be done in the future.

References

[1] W. U. Khan, M. A. Jamshed, A. Mahmood, E. Lagunas, S. Chatzinotas, and B. Ottersten, "Backscatter-aided NOMA V2X communication under channel estimation errors," 2022, *arXiv:2202.01586*.

[2] D. Jiang, L. Huo, Z. Lv, H. Song, and W. Qin, "A joint multi-criteria utility-based network selection approach for vehicle-to-infrastructure networking," *IEEE Trans. Intell. Transp. Syst.*, vol. 19, no. 10, pp. 3305–3319, Oct. 2018.

[3] S. Raza, S. Wang, M. Ahmed, M. R. Anwar, M. A. Mirza, and W. U. Khan, "Task offloading and resource allocation for IoV using 5G NR-V2X communication," *IEEE Internet Things J.*, vol. 9, no. 13, pp. 10397–10410, Jul. 2021.

[4] Z. Ali, W. U. Khan, A. Ihsan, O. Waqar, G. A. S. Sidhu, and N. Kumar, "Optimizing resource allocation for 6G NOMA-enabled cooperative vehicular networks," *IEEE Open J. Intell. Transp. Syst.*, vol. 2, pp. 269–281, 2021.

[5] M. Noor-A-Rahim *et al.*, "6G for vehicle-to-everything (V2X) communications: Enabling technologies, challenges, and opportunities," *Proc. IEEE*, vol. 110, no. 6, pp. 712–734, Jun. 2022.

[6] S. Gyawali, S. Xu, Y. Qian, and R. Q. Hu, "Challenges and solutions for cellular based V2X communications," *IEEE Commun. Surveys Tuts.*, vol. 23, no. 1, pp. 222–255, 1st Quart., 2021.

[7] J. Wang, K. Zhu, and E. Hossain, "Green Internet of vehicles (IoV) in the 6G era: Toward sustainable vehicular communications and networking," *IEEE Trans. Green Commun. Netw.*, vol. 6, no. 1, pp. 391–423, Mar. 2022.

[8] M. M. Saad, M. T. R. Khan, S. H. A. Shah, and D. Kim, "Advancements in vehicular communication technologies: C-V2X and NR-V2X comparison," *IEEE Commun. Mag.*, vol. 59, no. 8, pp. 107–113, Aug. 2021.

[9] W. Li and H. Song, "ART: An attack-resistant trust management scheme for securing vehicular ad hoc networks," *IEEE Trans. Intell. Transp. Syst.*, vol. 17, no. 4, pp. 960–969, Apr. 2016.

[10] C. Wang, C. Chen, Q. Pei, N. Lv, and H. Song, "Popularity incentive caching for vehicular named data networking," *IEEE Trans. Intell. Transp. Syst.*, vol. 23, no. 4, pp. 3640–3653, Apr. 2022.

[11] F. Zabini, A. Bazzi, B. M. Masini, and R. Verdone, "Optimal performance versus fairness tradeoff for resource allocation in wireless systems," *IEEE Trans. Wireless Commun.*, vol. 16, no. 4, pp. 2587–2600, Apr. 2017.

[12] A. Mukhopadhyay and G. Das, "Low complexity fair scheduling in LTE/LTE—A uplink involving multiple traffic classes," *IEEE Syst. J.*, vol. 15, no. 2, pp. 1616–1627, Jun. 2020.

[13] W. U. Khan, F. Jameel, T. Ristaniemi, S. Khan, G. A. S. Sidhu, and J. Liu, "Joint spectral and energy efficiency optimization for downlink NOMA networks," *IEEE Trans. Cognit. Commun. Netw.*, vol. 6, no. 2, pp. 645–656, Jun. 2020.

[14] Y. Liu, W. Yi, Z. Ding, X. Liu, O. Dobre, and N. Al-Dhahir, "Developing NOMA to next generation multiple access (NGMA): Future vision and research opportunities," 2021, *arXiv:2103.02334*.

[15] F. Zhang, M. M. Wang, X. Bao, and W. Liu, "Centralized resource allocation and distributed power control for NOMA-integrated NR V2X," *IEEE Internet Things J.*, vol. 8, no. 22, pp. 16522–16534, Nov. 2021.

[16] D. K. Patel *et al.*, "Performance analysis of NOMA in vehicular communications over i.n.i.d Nakagami-*m* fading channels," *IEEE Trans. Wireless Commun.*, vol. 20, no. 10, pp. 6254–6268, Oct. 2021.

[17] W. U. Khan, J. Liu, F. Jameel, V. Sharma, R. Jäntti, and Z. Han, "Spectral efficiency optimization for next generation NOMA-enabled IoT networks," *IEEE Trans. Veh. Technol.*, vol. 69, no. 12, pp. 15284–15297, Dec. 2020.

[18] Z. Ali *et al.*, "Fair power allocation in cooperative cognitive systems under NOMA transmission for future IoT networks," *Alexandria Eng. J.*, vol. 61, no. 1, pp. 575–583, 2022.

[19] T. Wang, Z. Qu, Z. Yang, T. Nichol, G. Clarke, and Y.-E. Ge, "Climate change research on transportation systems: Climate risks, adaptation and planning," *Transp. Res. D, Transp. Environ.*, vol. 88, Nov. 2020, Art. no. 102553.

[20] Y. Su, M. LiWang, L. Huang, X. Du, and N. Guizani, "Green communications for future vehicular networks: Data compression approaches, opportunities, and challenges," *IEEE Netw.*, vol. 34, no. 6, pp. 184–190, Nov./Dec. 2020.

[21] S. C. Kwan and J. H. Hashim, "A review on co-benefits of mass public transportation in climate change mitigation," *Sustain. Cities Soc.*, vol. 22, pp. 11–18, Apr. 2016.

[22] T. D. P. Perera, D. N. K. Jayakody, S. Chatzinotas, and J. Li, "Simultaneous wireless information and power transfer (SWIPT): Recent advances and future challenges," *IEEE Commun. Surveys Tuts.*, vol. 20, no. 1, pp. 264–302, 1st Quart., 2018.

[23] F. Jameel, S. Zeb, W. U. Khan, S. A. Hassan, Z. Chang, and J. Liu, "NOMA-enabled backscatter communications: Toward battery-free IoT networks," *IEEE Internet Things Mag.*, vol. 3, no. 4, pp. 95–101, Dec. 2020.

[24] W. U. Khan *et al.*, "Integration of backscatter communication with multi-cell NOMA: A spectral efficiency optimization under imperfect SIC," 2021, *arXiv:2109.11509*.

[25] H. Tran-Dinh, S. Gautam, S. Chatzinotas, and B. Ottersten, "Throughput maximization for wireless communication systems with backscatter- and cache-assisted UAV technology," 2020, *arXiv:2011.07955*.

[26] P. X. Nguyen *et al.*, "Backscatter-assisted data offloading in OFDMA-based wireless-powered mobile edge computing for IoT networks," *IEEE Internet Things J.*, vol. 8, no. 11, pp. 9233–9243, Jun. 2021.

[27] X. Li *et al.*, "Physical layer security of cognitive ambient backscatter communications for green Internet-of-Things," *IEEE Trans. Green Commun. Netw.*, vol. 5, no. 3, pp. 1066–1076, Sep. 2021.

[28] W. U. Khan *et al.*, "Learning-based resource allocation for backscatter-aided vehicular networks," *IEEE Trans. Intell. Transp. Syst.*, early access, Nov. 18, 2021, doi: 10.1109/TITS.2021.3126766.

[29] K. Zhu, L. Xu, and D. Niyato, "Distributed resource allocation in RF-powered cognitive ambient backscatter networks," *IEEE Trans. Green Commun. Netw.*, vol. 5, no. 4, pp. 1657–1668, Dec. 2021.

[30] F. Jameel, W. U. Khan, S. T. Shah, and T. Ristaniemi, "Towards intelligent IoT networks: Reinforcement learning for reliable backscatter communications," in *Proc. IEEE Globecom Workshops (GC Wkshps)*, Dec. 2019, pp. 1–6.

[31] Q. Zhang, L. Zhang, Y.-C. Liang, and P. Y. Kam, "Backscatter-NOMA: A symbiotic system of cellular and Internet-of-Things networks," *IEEE Access*, vol. 7, pp. 20000–20013, 2019.

[32] S. Zeb *et al.*, "NOMA enhanced backscatter communication for green IoT networks," in *Proc. 16th Int. Symp. Wireless Commun. Syst. (ISWCS)*, Aug. 2019, pp. 640–644.

[33] A. Farajzadeh, O. Ercetin, and H. Yanikomeroglu, "UAV data collection over NOMA backscatter networks: UAV altitude and trajectory optimization," in *Proc. IEEE Int. Conf. Commun. (ICC)*, May 2019, pp. 1–7.

[34] W. Chen, H. Ding, S. Wang, D. B. da Costa, F. Gong, and P. H. J. Nardelli, "Backscatter cooperation in NOMA communications systems," *IEEE Trans. Wireless Commun.*, vol. 20, no. 6, pp. 3458–3474, Jun. 2021.

[35] A. W. Nazar, S. A. Hassan, H. Jung, A. Mahmood, and M. Gidlund, "BER analysis of a backscatter communication system with non-orthogonal multiple access," *IEEE Trans. Green Commun. Netw.*, vol. 5, no. 2, pp. 574–586, Jun. 2021.

[36] X. Li, M. Zhao, Y. Liu, L. Li, Z. Ding, and A. Nallanathan, "Secrecy analysis of ambient backscatter NOMA systems under I/Q imbalance," *IEEE Trans. Veh. Technol.*, vol. 69, no. 10, pp. 12286–12290, Oct. 2020.

[37] A. Raza *et al.*, "A NOMA-enabled cellular symbiotic radio for mMTC," *Wireless Pers. Commun.*, vol. 122, no. 4, pp. 1–27, 2021.

[38] X. Li *et al.*, "Cognitive AmBC-NOMA IoV-MTS networks with IQI: Reliability and security analysis," *IEEE Trans. Intell. Transp. Syst.*, early access, Sep. 27, 2021, doi: 10.1109/TITS.2021.3113995.

[39] Z. Ding, "Harvesting devices' heterogeneous energy profiles and QoS requirements in IoT: WPT-NOMA vs BAC-NOMA," *IEEE Trans. Commun.*, vol. 69, no. 5, pp. 2837–2850, May 2021.

[40] X. Li *et al.*, "Hardware impaired ambient backscatter NOMA systems: Reliability and security," *IEEE Trans. Commun.*, vol. 69, no. 4, pp. 2723–2736, Apr. 2021.

[41] C.-B. Le, D.-T. Do, X. Li, Y.-F. Huang, H.-C. Chen, and M. Voznak, "Enabling NOMA in backscatter reconfigurable intelligent surfaces-aided systems," *IEEE Access*, vol. 9, pp. 33782–33795, 2021.

[42] W. U. Khan, M. A. Javed, T. N. Nguyen, S. Khan, and B. M. Elhalawany, "Energy-efficient resource allocation for 6G backscatter-enabled NOMA IoV networks," *IEEE Trans. Intell. Transp. Syst.*, early access, Sep. 21, 2021, doi: 10.1109/TITS.2021.3110942.

[43] Y. Liao, G. Yang, and Y.-C. Liang, "Resource allocation in NOMA-enhanced full-duplex symbiotic radio networks," *IEEE Access*, vol. 8, pp. 22709–22720, 2020.

[44] W. U. Khan, F. Jameel, N. Kumar, R. Jantti, and M. Guizani, "Backscatter-enabled efficient V2X communication with non-orthogonal multiple access," *IEEE Trans. Veh. Technol.*, vol. 70, no. 2, pp. 1724–1735, Feb. 2021.

[45] Z. Ding and H. V. Poor, "Advantages of NOMA for multi-user BackCom networks," *IEEE Commun. Lett.*, vol. 25, no. 10, pp. 3408–3412, Oct. 2021.

[46] W. U. Khan, N. Imtiaz, and I. Ullah, "Joint optimization of NOMA-enabled backscatter communications for beyond 5G IoT networks," *Internet Technol. Lett.*, vol. 4, no. 2, p. e265, Mar. 2021.

[47] W. U. Khan, X. Li, M. Zeng, and O. A. Dobre, "Backscatter-enabled NOMA for future 6G systems: A new optimization framework under imperfect SIC," *IEEE Commun. Lett.*, vol. 25, no. 5, pp. 1669–1672, May 2021.

[48] Y. Xu, Z. Qin, G. Gui, H. Gacanin, H. Sari, and F. Adachi, "Energy efficiency maximization in NOMA enabled backscatter communications with QoS guarantee," *IEEE Wireless Commun. Lett.*, vol. 10, no. 2, pp. 353–357, Feb. 2021.

[49] W. U. Khan, Z. Ali, A. U. Khan, and G. A. S. Sidhu, "Secure backscatter-enabled NOMA system design in 6G era," *Internet Technol. Lett.*, vol. 4, no. 6, p. e307, Nov. 2021.

[50] W. U. Khan, J. Liu, F. Jameel, M. T. R. Khan, S. H. Ahmed, and R. Jäntti, "Secure backscatter communications in multi-cell NOMA networks: Enabling link security for massive IoT networks," in *Proc. Conf. Comput. Commun. Workshops (INFOCOM WKSHPS)*, Jul. 2020, pp. 213–218.

[51] Z. Ding and H. V. Poor, "On the application of BAC-NOMA to 6G umMTC," *IEEE Commun. Lett.*, vol. 25, no. 8, pp. 2678–2682, Aug. 2021.

[52] M. Ahmed, W. U. Khan, A. Ihsan, X. Li, J. Li, and T. A. Tsiftsis, "Backscatter sensors communication for 6G low-powered NOMA-enabled IoT networks under imperfect SIC," 2021, *arXiv:2109.12711*.

[53] W. U. Khan, F. Jameel, A. Ihsan, O. Waqar, and M. Ahmed, "Joint optimization for secure ambient backscatter communication in NOMA-enabled IoT networks," *Digit. Commun. Netw.*, early access, Mar. 2022.

[54] W. U. Khan, F. H. Memon, K. Dev, M. A. Javed, D.-T. Do, and N. M. F. Qureshi, "Ambient BackCom in beyond 5G NOMA networks: A multi-cell resource allocation framework," *TechRxiv*, pp. 1–10, 2021.

[55] S. Boyd, S. P. Boyd, and L. Vandenberghe, *Convex Optimization*. Cambridge, U.K.: Cambridge Univ. Press, 2004.

Wali Ullah Khan (Member, IEEE) received the master's degree in electrical engineering from COMSATS University Islamabad, Pakistan, in 2017, and the Ph.D. degree in information and communication engineering from Shandong University, Qingdao, China, in 2020. He is currently working with the Interdisciplinary Centre for Security, Reliability and Trust (SnT), University of Luxembourg, Luxembourg. He has authored/coauthored more than 70 publications, including international journals, peer-reviewed conferences, and book chapters. His research interests include convex/nonconvex optimizations, non-orthogonal multiple access, reflecting intelligent surfaces, ambient backscatter communications, the Internet of Things, intelligent transportation systems, satellite communications, unmanned aerial vehicles, physical layer security, and applications of machine learning.

Muhammad Ali Jamshed (Member, IEEE) received the B.Sc. degree in electrical engineering from COMSATS University Islamabad, Islamabad, Pakistan, in 2013, the M.Sc. degree in wireless communications from the Institute of Space Technology, Islamabad, in 2016, and the Ph.D. degree from the University of Surrey, Guildford, U.K., in 2021. He served briefly as a Wireless Research Engineer with BriteYellow Ltd., U.K.; and then moved to the James Watt School of Engineering, University of Glasgow, as a Research Assistant. His main research interests include EMF exposure reduction, low SAR antennas for mobile handsets, backscatter communication, and wireless sensor networks. He was nominated for the Departmental Prize for Excellence in Research in 2019 at the University of Surrey.

Eva Lagunas (Senior Member, IEEE) received the M.Sc. and Ph.D. degrees in telecommunications engineering from the Polytechnic University of Catalonia (UPC), Barcelona, Spain, in 2010 and 2014, respectively. From 2009 to 2013, she was a Research Assistant with the Department of Signal Theory and Communications, UPC. In 2009, she was a Guest Research Assistant with the Department of Information Engineering, University of Pisa, Pisa, Italy. From November 2011 to May 2012, she held a visiting research appointment with the Center for Advanced Communications, Villanova University, PA, USA. In 2014, she joined the Interdisciplinary Centre for Security, Reliability and Trust (SnT), University of Luxembourg, Luxembourg, where she currently holds a Research Scientist position. Her research interests include radio resource management and general wireless networks optimization.

Symeon Chatzinotas (Senior Member, IEEE) received the M.Eng. degree in telecommunications from the Aristotle University of Thessaloniki, Thessaloniki, Greece, in 2003, and the M.Sc. and Ph.D. degrees in electronic engineering from the University of Surrey, Guildford, U.K., in 2006 and 2009, respectively. He is currently a Full Professor or the Chief Scientist I and the Co-Head of the Interdisciplinary Centre for Security, Reliability and Trust, SIGCOM Research Group, University of Luxembourg. In the past, he was a Visiting Professor with the University of Parma, Parma, Italy; and he was involved in numerous research and development projects for the National Center for Scientific Research Demokritos; the Center of Research and Technology, Hellas; and the Center of Communication Systems Research, University of Surrey. He has coauthored more than 400 technical papers in refereed international journals, conferences, and scientific books. He was the co-recipient of the 2014 IEEE Distinguished Contributions to Satellite Communications Award, the CROWNCOM 2015 Best Paper Award, and the 2018 *EURASIP JWCN* Best Paper Award. He is currently on the Editorial Board of the IEEE OPEN JOURNAL OF VEHICULAR TECHNOLOGY and the *International Journal of Satellite Communications and Networking*.

Xingwang Li (Senior Member, IEEE) received the M.Sc. degree from the University of Electronic Science and Technology of China in 2010 and the Ph.D. degree from the Beijing University of Posts and Telecommunications in 2015. From 2010 to 2012, he worked with Comba Telecom Ltd., Guangzhou, China, as an Engineer. He spent one year from 2017 to 2018 as a Visiting Scholar at Queen's University Belfast, Belfast, U.K. He is also a Visiting Scholar with the State Key Laboratory of Networking and Switching Technology, Beijing University of Posts and Telecommunications, from 2016 to 2018. He is currently an Associate Professor with the School of Physics and Electronic Information Engineering, Henan Polytechnic University, Jiaozuo, China. His research interests include MIMO communication, cooperative communication, hardware constrained communication, non-orthogonal multiple access, physical layer security, unmanned aerial vehicles, and the Internet of Things. He has served as a TPC Member for the IEEE GLOBECOM, IEEE WCNC, IEEE VTC, and IEEE ICCC. He has also served as the Co-Chair for the IEEE/IET CSNDSP 2020 of the Green Communications and Networks Track. He also serves as an Editor on the Editorial Board for IEEE ACCESS, *Computer Communications*, *Physical Communication*, *KSII Transactions on Internet and Information Systems*, and *IET Quantum Communication*. He is also the Lead Guest Editor for the Special Issue on UAV-Enabled B5G/6G Networks: Emerging Trends and Challenges of *Physical Communication*, the Special Issue on Recent Advances in Physical Layer Technologies for the 5G-Enabled Internet of Things of *Wireless Communications and Mobile Computing*, and the Special Issue on Recent Advances in Multiple Access for 5G-Enabled IoT of *Security and Communication Networks*.

Björn Ottersten (Fellow, IEEE) was born in Stockholm, Sweden, in 1961. He received the M.S. degree in electrical engineering and applied physics from Linköping University, Linköping, Sweden, in 1986, and the Ph.D. degree in electrical engineering from Stanford University, Stanford, CA, USA, in 1990. He has held research positions with the Department of Electrical Engineering, Linköping University; the Information Systems Laboratory, Stanford University; the Katholieke Universiteit Leuven, Leuven, Belgium; and the University of Luxembourg, Esch-sur-Alzette, Luxembourg. From 1996 to 1997, he was the Director of Research with ArrayComm Inc., a start-up in San Jose, CA, USA, based on his patented technology. In 1991, he was appointed as a Professor of signal processing with the Royal Institute of Technology (KTH), Stockholm. He has been the Head of the Department for Signals, Sensors, and Systems, KTH; and the Dean of the School of Electrical Engineering, KTH. He is currently the Director for the Interdisciplinary Centre for Security, Reliability and Trust, University of Luxembourg. He is currently a member of the Editorial Board of the IEEE OPEN JOURNAL OF SIGNAL PROCESSING, *EURASIP Signal Processing Journal*, *EURASIP Journal on Advances in Signal Processing*, and *Foundations and Trends in Signal Processing*. He is a fellow of EURASIP. He was the recipient of the IEEE Signal Processing Society Technical Achievement Award and been twice awarded the European Research Council Advanced Research Grant. He has coauthored journal articles which was the recipient of the IEEE Signal Processing Society Best Paper Award in 1993, 2001, 2006, 2013, and 2019; and eight IEEE conference papers best paper awards. He has been a Board Member of IEEE Signal Processing Society and the Swedish Research Council and currently serves on the Boards of EURASIP and the Swedish Foundation for Strategic Research. He was an Associate Editor of the IEEE TRANSACTIONS ON SIGNAL PROCESSING and the Editorial Board of the *IEEE Signal Processing Magazine*.